**EXAMINING IMPACT DISRUPTION CRITERIA FOR MID-SIZED ICY BODIES.**

Naor Movshovitz[1] (nmovshov@ucsc.edu), Francis Nimmo[1], Don Korycasnky[1], and Erik Asphaug[2].
[1]Earth and Planetary Sciences, University of California Santa Cruz, 1156 High Street, Santa Cruz, CA 95064
[2]School of Earth and Space Exploration, Arizona State University, Tempe, AZ

**Introduction:** The ability to predict the outcome of collision between planetary bodies is crucial for our understanding of the origin and evolution of the solar system (e.g. [1]–[3]). In the context of planetary accretion, for example, the most basic question to answer is whether a collision leads to net accretion or net erosion of the colliding system. The mass of the largest post-collision gravitationally bound fragment, $M_{\mathrm{lr}}$, is for this reason the focus of attention.

In this work we apply a similar formalism as in [4] to collision outcomes from a set of consistent SPH simulations. With an eye towards applications in early planet and satellite formation [1], [3] we focus on icy bodies with radii between 100 and 3000 km. We provide a scaling law that interpolates, rather than extrapolates in this size regime and is able to better reproduce simulated results.

**Overview:** To determine $M_{\mathrm{lr}}$ for a particular collision requires numerical integration of, at least, the hydrodynamic equations for the colliding material. For bodies smaller than ~10 km radius elastic strength and the details of mechanical fracturing are important and must be simulated as well, while for larger targets gravity is the dominant force and the trajectories of post-collision fragments must be integrated long enough to allow for gravitational re-accumulation. As this requires significant computational effort, it is important to find efficient ways to extrapolate from the results of specific numerical simulations to collisions that are nearby in parameter space.

A collision scenario is completely identified by the target and projectile radii, $R$ and $r$, the target and projectile masses, $m_t$ and $m_p$, and the impact speed $V_i$ and impact parameter $b$. A useful approach has been to focus on the kinetic energy of impact normalized by the target mass or total colliding mass. Many studies have shown that $M_{\mathrm{lr}}$ is simply related to this specific energy, $Q$, when normalized by a critical value $Q_{\mathrm{D}}^*$ that depends on the target, and have suggested scaling laws to predict $Q_{\mathrm{D}}^*$ for targets of various sizes and compositions [3], [5]–[10].

Recently in [4] Leinhardt and Stewart attempted to synthesize results from a large number of studies by converting critical disruption values obtained with different impact angles, impact speeds, and projectile-to-target mass ratios into equivalent values for head-on impacts between similar sized bodies, characterized by the total mass and material alone. The advantage of this approach is that data from many previous studies can be used to construct best-fit curves for this type of collision. The authors call these *principal disruption curves*, and use them to predict the critical disruption energy for an arbitrary collision. But as different studies typically use different computer codes with different setup and post-processing requirements the data is inevitably more scattered, and the best-fit curves derived from the global data set are not necessarily the ones that best reproduce the results in any subset of available data. For instance, we find that the principal disruption curves of [4] typically overestimate the energy required to disrupt icy targets with $R > 500$ km by a factor of 5 or more [3].

**Method:** We simulate impacts into hydrostatic ice targets using the SPH-based hydro-code SPHERAL [11], [12]. For each target we use several mass ratios of projectiles and vary the impact speed to find the critical value $V^*$ for which $M_{\mathrm{lr}}$ is half the total colliding mass, $M_{\mathrm{tot}}$. We determine $M_{\mathrm{lr}}$ by applying an iterative energy balance algorithm [5]. We then interpolate between the runs with $M_{\mathrm{lr}}/M_{\mathrm{tot}}$ values nearest to 0.5 to determine $V^*$.

To construct the principal disruption curves (PDC) we follow a procedure similar to that in [4] (modified only in the treatment of oblique impacts). The formalism calls for using the variable

$$Q_{\mathrm{R}} = \frac{1}{2}\frac{m_t m_p}{\left(m_t + m_p\right)^2} V_i^2 \tag{1}$$

to describe the collision. The ratio $m_p/m_p$ is denoted by $\gamma$ and the critical value of $Q_{\mathrm{R}}$ that corresponds to $V_i = V^*$ is denoted $Q_{\mathrm{RD}}^*$.

Values of $Q_{\mathrm{RD}}^*$ obtained for different values of $\gamma$ need to be converted to the equivalent energy for a collision of equal mass bodies. The scaling suggested in [4],

$$Q_{\mathrm{RD}}^* \propto R_{\mathrm{c1}}^{3\bar{\mu}} V^{*(2-3,\bar{u})} \tag{2}$$

uses the variable $R_{\mathrm{c1}}$, the radius of a sphere of density $\rho_1 = 1000\ \mathrm{kg\ m^{-3}}$ containing the total colliding mass, and $\bar{\mu}$ the coupling parameter introduced in [13]. Taken together eqs. (1) and (2) imply (sec. 3 of [4]), first, that for a fixed mass ratio $Q_{\mathrm{RD}}^* \propto R_{\mathrm{c1}}^2$ and, second, that the critical energy for any value of $\gamma$ is related to the critical energy at $\gamma = 1$ by

$$Q_{\mathrm{RD}}^* = Q_{\mathrm{RD},\gamma=1}^* \left(\frac{1}{4}\frac{(\gamma+1)^2}{\gamma}\right)^{\left(\frac{2}{3\bar{\mu}}-1\right)}. \tag{3}$$

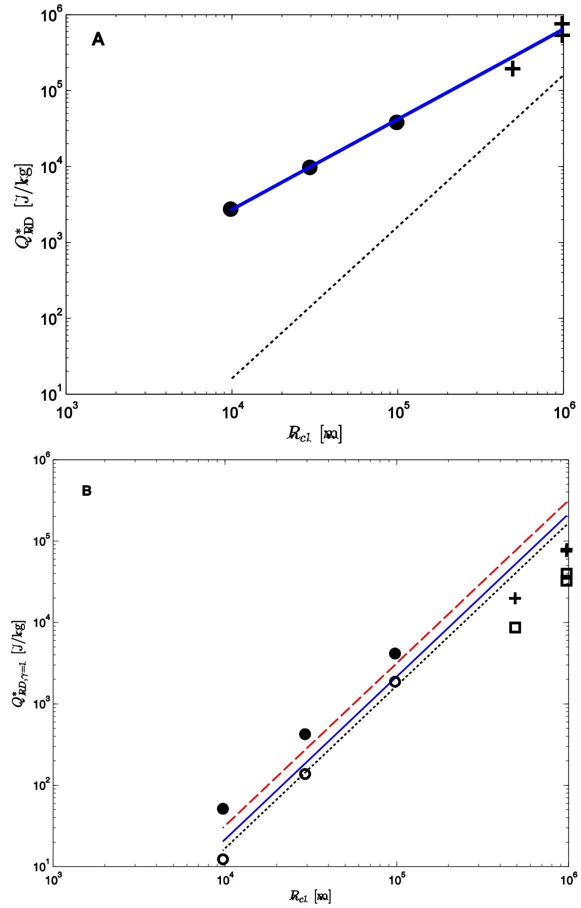


**Figure 1.** Critical disruption energy derived from SPH simulations of impacts between gravity-dominated ice targets. (A) Values derived from impacts with different projectile-to-target mass ratios. Plus markers: data from our simulations; filled circles: data from [5] high velocity runs with ice targets. Dotted line shows the approximate gravitational binding energy *U* and the solid blue line shows the $Q^*_D \propto R^{1.28}$ scaling found in [3, 5]. (B) Same data converted to the critical energy required to disrupt the equivalent system with equal-mass target and projectile, using eq. (3) with $\bar{\mu} = 0.4$. Solid blue line is the best-fit PDC (eq. (4)) with $c^* = 1.3$. Also shown in open squares and open circles are the same data converted using the value $\bar{\mu} = 0.35$ recommended in [4]. Dashed red line is the PDC for weak targets in [4].

Therefore, when plotted against $R_{c1}$ on a log scale the equivalent equal-mass disruption energies should fall on the same line of slope 2. We use this fact to find a best-fit value of $\bar{\mu}$.

Then, as $Q^*_{RD,\gamma=1} \propto R^2_{c1}$ and is close in value to the gravitational binding energy, we try to fit

$$Q^*_{RD,\gamma=1} = c^* \frac{4}{5} \pi \rho_1 G R^2_{c1}. \quad (4)$$

With the parameters $c^*$ and $\bar{\mu}$ we can then predict $Q^*_{RD}$ and therefore $M_{lr}$ for a collision with any initial conditions.

**Preliminary results:** In figure 1 we show the results of simulations completed to date. The $M_{lr}/M_{tot}$ values of several runs were used to derive a $Q^*_{RD}$ value for two projectile-to-target mass ratios. Three more values are taken from [5] where smaller targets were used in simulations using a similar SPH code. In Fig. 1A the critical disruption energy is plotted against $R_{c1}$, and in Fig. 1B the equivalent values for equal-mass collision are plotted, using $\bar{\mu} = 0.4$.

Data from the same set of simulations always fall on a line of slope 2 when converted to equal-mass disruption energies. But the two subsets fall on lines that are separated by a constant offset. This may indicate a non-physical dissipation mechanism in one or both of the codes. For this reason, the best-fit principal disruption curve, with $c^* = 1.3$, is not a very good fit for either of the subsets individually.

For comparison we also plot in Fig. 1B the same data converted to equal-mass disruption energies using the value $\bar{\mu} = 0.35$ recommended in [4], and the corresponding principal disruption curve with $c^* = 1.9$. As these values were designed to fit even more data from other sources, they result in an even worse fit for each subset of data.

It is worth noting that the *uncorrected* values in Fig. 1A still follow a power-law very closely, albeit one with a shallower slope. This is the equivalent of assuming $\bar{\mu} = 2/3$ or pure energy scaling. This is also consistent with the findings in [5] and taken together with the output from our simulations suggests that the critical disruption energy scales with $R^{1.188}$. The shallower slope suggests that in the limit of large targets the disruption energy will approach the gravitational binding energy.

**References:** **[1]** C. Dwyer, F. Nimmo, M. Ogihara, and S. Ida, *Icarus*, vol. 225, no. 1, pp. 390–402, Jul. 2013. **[2]** J. E. Chambers, *Icarus*, vol. 224, no. 1, pp. 43–56, May 2013. **[3]** N. Movshovitz, D. Korycansky, F. Nimmo, E. Asphaug, and J. Owen, in *Lunar and Planetary Institute Science Conference Abstracts*, 2014, pp. 1–2. **[4]** Z. M. Leinhardt and S. T. Stewart, *Astrophys. J.*, vol. 745, no. 1, p. 79, Jan. 2012. **[5]** W. Benz and E. Asphaug, *Icarus*, vol. 142, pp. 5–20, 1999. **[6]** K. A. Holsapple, *Annu. Rev. Earth Planet. Sci.*, vol. 21, pp. 333–373, 1993. **[7]** K. A. Holsapple, I. Giblin, K. R. Housen, A. Nakamura, and E. Ryan, in *Asteroids III*, W. F. Bottke, A. Cellino, P. Paolicchi, and R. Binzel, Eds. Tucson: University of Arizona Press, 2002, pp. 443–462. **[8]** S. T. Stewart and Z. M. Leinhardt, *Astrophys. J.*, vol. 691, no. 2, pp. L133–L137, Feb. 2009. **[9]** R. Marcus, D. Sasselov, S. T. Stewart, and L. Hernquist, *Astrophys. J. Lett.*, vol. 719, pp. L45–L49, Aug. 2010. **[10]** M. Jutzi, P. Michel, W. Benz, and D. C. Richardson, *Icarus*, vol. 207, no. 1, pp. 54–65, May 2010. **[11]** J. Owen, J. Villumsen, P. Shapiro, and H. Martel, *Astrophys. J. Suppl. Ser.*, vol. 116, pp. 155–209, 1998. **[12]** J. Owen, in *5th International SPHERIC SPH Workshop*, 2010, pp. 297–304. **[13]** K. R. Housen and K. A. Holsapple, *Icarus*, vol. 84, pp. 226–253, 1990.